

## Review on Strain Sensors for detection of Human Facial Expressions Recognition Systems

Noor Amalina Ramli<sup>1</sup>, Anis Nurashikin Nordin<sup>1\*</sup> and Norsinnira Zainul Azlan<sup>2</sup>

<sup>1</sup> *Electrical and Computer Engineering Department, Kulliyah of Engineering, International Islamic University Malaysia, Jalan Gombak, 53100, Kuala Lumpur, Malaysia.*

<sup>2</sup> *Mechatronics Department, Kulliyah of Engineering, International Islamic University Malaysia, Jalan Gombak, 53100, Kuala Lumpur, Malaysia.*

Received 21 January 2020, Revised 26 February 2020, Accepted 12 June 2020

### ABSTRACT

*Facial expression plays an important factor in human communication which helps us to understand the intentions and emotions of others. Generally, people infer the emotional states of other people such as fear, sadness, joy and anger just by looking at the facial expression and vocal tone. Moreover, facial expression can also be used to deliver messages especially for those who are paralyzed which their only means of communication is through facial expression. Therefore, by exploiting the facial expression of a paralyzed patient, a sensory system could be developed which would allow the patient to communicate with others and to assist them to actuate robotic limbs in order to improve their mobility. Conventional methods such as vision sensors that use cameras to detect facial expression have suffered from low mobility, high complexity, high cost and difficulty to adapt as wearable. Stretchable electronic devices have been developed for various applications including heaters, energy converters, transistors and sensors. Wearability, conformability to the skin, less complicated design and low cost promotes the use of strain sensor as part of a system for facial expression detection. This review paper presents the development of stretchable strain sensors for human facial expression detection focusing mainly on the materials and fabrication strategies. In addition, this paper also provides fundamental structural design as well as challenges and opportunities in realizing stretchable strain sensor and their various potential applications.*

**Keywords:** Facial Expression Recognition, Stretchable Strain Sensor, Wearables.

### 1. INTRODUCTION

One of the basic methods for humans to communicate their emotions is by using facial expression. Facial expression differs depending on the perceived situations which can range from pleasant to dangerous. The state and emotion of a person can be interpreted by others which can be very helpful especially if that person is unable to convey his or her emotion verbally. The inability to speak could be due to several medical conditions such as stroke, multiple sclerosis and Alzheimer which cause a person to lose the ability to move one or more muscles of the body. Previously, studies of facial expression were only carried out by psychologists in order to understand human behaviour. However, this phenomenon has changed over the past decades in line with the advancement of technology. As a result, applications of Facial Expression Recognition (FER) have been expanded to different disciplines and areas such as health care monitoring [1], entertainment [2]–[4], robotic [5], human motion detection [6], [7], human-computer interface (HCI) [8], [9] and security systems [10] as

---

\*Corresponding Author: anisnn@iium.edu.my

depicted in Figure 1(a). For instance, the signals from the FER systems have been used to actuate smart robots as well as an input to lying detection systems. Although substantial progress has been achieved in this field to date, identifying human facial expression remains a challenge due to the subtlety, complexity and variability of human facial expressions [11].

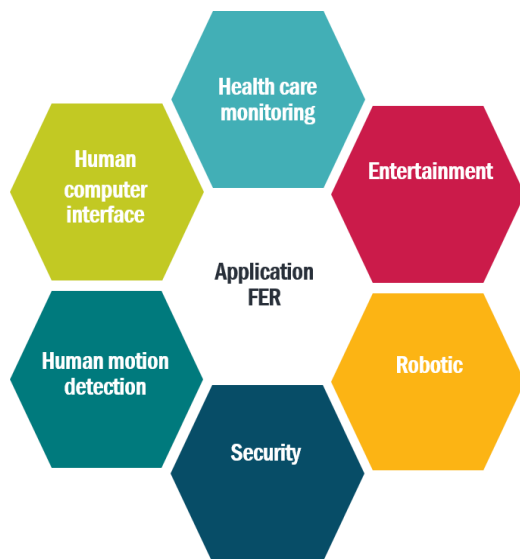


**Figure 1 (a).** Application of FER System.

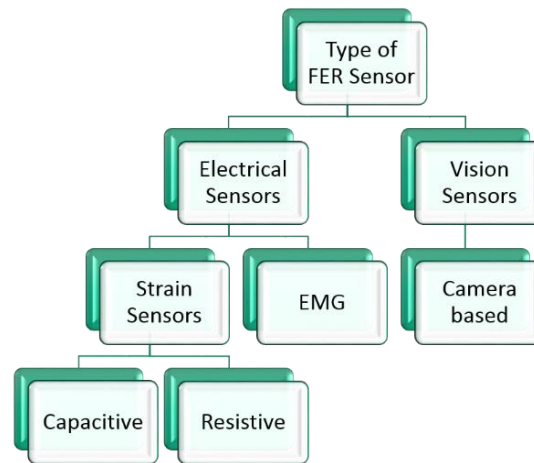


**Figure 1 (b).** Types of Sensors.

### 1.1 Types of Sensors

There are several types of state-of-the-art sensors that have been proposed to detect facial expression in the literature. These sensors can be categorized into two main categories which are vision sensors and electrical sensors as illustrated in Figure 1(b). Vision sensor such as camera-based sensor is the most commonly utilized sensor to recognize facial expression due to the readily available cameras in the market and ease of operation [12]–[19]. Moreover, it has high spatial resolution and sensitivity along with the unobtrusive feature which is lacking in other sensors [15]–[17]. However, vision sensor suffers from low mobility, high complexity, high cost and difficulty to adapt to wearable, patchable or implantable electronic which are found in numerous applications ranging from health monitoring to entertainment at the present time [18]–[20].

On the other hand, electrical sensors such as electromyogram (EMG), electrocardiography (ECG), electroencephalogram (EEG) and strain sensor have the potential to overcome the limitations of the vision sensor by capturing the FER input more efficiently. ECG and EEG operate specifically by acquiring the electrical activity of the heart and brain respectively over time using electrodes attached on the skin [21], [22]. In the case of the EMG sensor, a skin electrode which can detect electrical potential generated during muscle contraction is attached on certain parts of the body [23]–[26]. In theory, electrical currents are generated by the exchange of ions across the muscle fibre membranes. When muscle contracts, a negative voltage, or action potential, travels along the cell membrane where this potential can be detected and measured. Several advantages of EMG are high temporal resolutions, high sensitivity in capturing subtle facial muscle activities that are not visible, convenient for testing without the need for head adjustment, and easy to be embedded in wearable devices. However, the EMG sensor suffers from weak signals generated by the muscles due to noise and the complicated relationship between muscle contractions and the generated electrical currents [27]. Therefore, as an alternative approach to these electrical sensors, stretchable strain sensor can be adopted instead to detect a various range of strains induced on human skin. Its

conformability to the skin makes it patchable and more sensitive compared to the EMG approach. Strain sensors work by detecting the changes in electrical impedance due to the structural deformation of the sensors caused by muscle movements. To detect large strain during body movement such as walking, running and grasping, the strain sensor requires high stretchability performance while to detect small strain such as in the face, very sensitive sensors are needed.

## 1.2 Motivation

Despite the rapid advances in the development of facial expression recognition in the past few years, there are no comprehensive literature reviews discussing strain sensors for facial expression recognition. Most review papers in the literature focus solely on one particular approach for FER such as camera or electromyogram (EMG) [17][27][28]. Therefore, this paper is aimed to fill the gap by providing a comprehensive literature review of FER by looking at all the existing methods. Moreover, emphasis will be given to strain sensor by explaining its working principles, sensor designs, materials and fabrication methods. The article is organized as follows: Section 2 presents the theory and strain-responsive mechanism of strain sensors for FER. Section 3 highlights the classification of human facial expressions and the placements of strain sensors. In Section 4, materials and fabrication processes of strain sensors are summarized. Challenges and future works are discussed in Section 5 and conclusions are drawn in Section 6.

## 2. STRAIN SENSOR

### 2.1 Theory of Strain Sensor

In general, strain sensors are transducers that convert mechanical deformations into electrical signals. Strain sensors can be mainly classified into two groups based on the measured electrical parameters which are resistive-type strain sensor and capacitive-type strain sensors as shown in Figure 1(b). A resistive-type strain sensor responds to mechanical deformation from external force by changing its electrical resistance while a capacitive-type strain sensor experiences changes in its capacitance. The relationship between electrical resistances in conductive materials to its physical dimension can be described by equation (1) [29].

$$R = \rho \frac{l}{A} \quad (1)$$

where  $\rho$  is a resistivity,  $l$  is the length and  $A$  is the area. Meanwhile, the relationship between the capacitance of capacitive materials and its physical dimension can be calculated as [29]:

$$C = \frac{A\epsilon_o}{d} \quad (2)$$

where  $\epsilon_o$  is the dielectric constant of a material. As for facial expression recognition, resistive-type strain sensors are widely implemented compared to the capacitive-type due to higher sensitivity towards small scale mechanical deformation from facial gestures. The strain-induced by muscles in the face that causes the change of electrical resistance of the sensors is mainly due to the change of the conductor length. Therefore, by sensing the basic muscle movements on the human face, a smart facial expression recognition can be developed.

Stretchability, sensitivity or Gauge Factor ( $G_{fs}$ ), and linearity are the main performance parameter of strain sensors [29]. Moreover, the reliability of these sensors is another important parameter that should be characterized to ensure they can withstand large and frequent strains over their lifetime. The stretchability and sensitivity of a strain sensor vary depending on various factors such as types of materials used for the electrical conductor and substrate of the

sensor and the physical structures of the device. The stretchability of the device can be defined as [29]:

$$\varepsilon = \frac{l - l_0}{l_0} \quad (3)$$

where  $l$  is the length after applying the strain while  $l_0$  is the original length. Generally, the sensitivity of strain sensors can be measured using equation (4) for resistive-type sensors and equation (5) for capacitive-type sensors [29].

$$G_{fs} = \frac{\left(\frac{\Delta R}{R}\right)}{\varepsilon} \quad (4)$$

$$G_{fs} = \frac{\left(\frac{\Delta C}{C}\right)}{\varepsilon} \quad (5)$$

The  $\Delta R$  and  $\Delta C$  are the changes of resistance and capacitance when strains are induced for resistive and capacitive sensors respectively and  $\varepsilon$  is the permittivity of the material. A highly sensitive strain sensor will produce a large amount of resistance or capacitance change when the sensor is subjected to strain. In most cases, strain sensors are required to accommodate large strain which makes linearity as one of the important performance parameters. However, resistive-type strain sensors are known to be susceptible to non-linearity effect which occurs when the microstructure of thin films of the sensors undergoes change from homogenous morphology to non-homogenous morphology when large strain is applied [29]. Apart from performance parameter mentioned above, durability can also be considered as one of the figure of merit (FoM) for stretchable devices where it measures the ability of the strain sensor to recover its original properties after being subjected to the deformation due to applied strain [30].

## 2.2 Strain Sensing Mechanism

There are several responsive operations for strain sensors depending on the type of materials used and fabrication approach as presented in [29]. Conventional resistive strain sensors which are mostly made of metal and piezoresistive material experience changes in length and cross-sectional area due to the applied strain. Besides the dimensional change, the change in resistance of stretchable strain sensors also can be caused by materials disconnection, crack propagation and tunnelling effect mechanism [29].

### 2.2.1 Dimensional Change

Compared to other operations, the dimensional change caused by applied strain is the main mechanism of commercially available strain sensors. For the resistive-type strain sensors, the increase of the resistance is due to the increase in length and the shrinkage in the cross-sectional area of the conductor as described in equation (1). On the other hand, capacitive-type sensors experience an increase in capacitance when the capacitive area and the thickness of the dielectric layer are reduced as given in equation (2).

### 2.2.2 Piezoresistive Effect

Piezoresistivity is the change of resistance in a material due to the structural deformation. The relative change of resistance due to piezoresistivity can be represented by [29]:

$$\frac{\Delta R}{R} = (1 + 2\nu)\varepsilon + \frac{\Delta\rho}{\rho} \quad (6)$$

Based on equation (6), the change in resistance is caused by two factors which are dimensional change given in the first term of the expression and piezoresistivity given in the second part of the expression. To take full advantage of the effect of piezoresistivity, strain sensors were made of semiconductor and nanomaterials where the change in resistance can be of multiple order of magnitude compared to metal and metal alloy. However, these materials suffer from low stretchability ( $\epsilon \leq 5\%$ ) which limits their application in the skin mountable or wearable strain sensors which generally require high stretchability ( $\epsilon > 50\%$ ) [31].

### 2.2.3 Disconnection Mechanism

In this disconnection method, the conductive thin films of the strain sensors are synthesized from nanomaterial conductive networks such as silver nanowires (AgNWs) and graphene flakes [32][33][34]. In an unstretched sensor, electrons can flow through the overlapping nanowires structures within the conductive layer. However, when strain is applied to the sensors, the stretched structure causes some of the connected nanowires to lose their overlapped area hence increasing the conductor's resistance. As the sensors experience more strain, more disconnection between nanowires occurs which further led to an increase of resistance. Figure 2(a) and (b) show the effect of elongation on the microstructure of cotton-AgNW network before and under tensile strain [34].

### 2.2.4 Microcrack Propagation

The micro-cracks method has been widely applied in the fabrication of ultrasensitive strain sensors [35][36]. A thin film made of CNT, silver nanoparticle (AgNP), gold nanowire (AuNW) and graphene thin film is typically coated on a flexible substrate such as PDMS [37]. By stretching the sensor, the original cracks which exist to release the stress in the film start to open and become large thus significantly increase the electrical resistance. As the strain is removed, microcracks start to heal and reconnect causing the resistance of the sensors to decrease to its original value. Figure 2(c) and (d) show the micro-cracks on the Ag NP thin film at  $\epsilon = 0\%$  and  $\epsilon = 20\%$  [36].

### 2.2.5 Tunneling Effect

Another mechanism that causes the resistance of strain sensors to increase is due to the tunnelling effect [29][38]. The ability of electrons to cross a nonconductive barrier is called tunnelling. For strain sensors made of CNTs-polymer nanocomposites, very thin insulating layers are formed that cause several CNT-CNT junctions to be electrically separated [39]. However, due to the tunnelling effect, the electrical conduction within the film is still possible. The cut-off tunnelling distance which varies among conductive materials and processing methods limits electrical conduction within the sensors. For instance, AgNW-PDMS-AgNW has the tunnelling cut-off distance of 0.58 nm. The resistance change due to the tunnelling effect can be presented by Simmons' theory where  $A$  is the cross-section of tunnelling junction,  $J$  is the tunnelling current density,  $V$  is the electrical potential difference,  $h$  is Plank constant,  $d$  distance between adjacent nanomaterials,  $e$  is the single-electron charge,  $m$  is the mass of an electron and  $\lambda$  is the height of energy barrier for polymer [29].

$$R_{tunnel} = \frac{V}{AJ} = \frac{h^2 d}{Ae^2 \sqrt{2m\lambda}} \exp\left(\frac{4\pi d}{h} \sqrt{2m\lambda}\right) \quad (7)$$

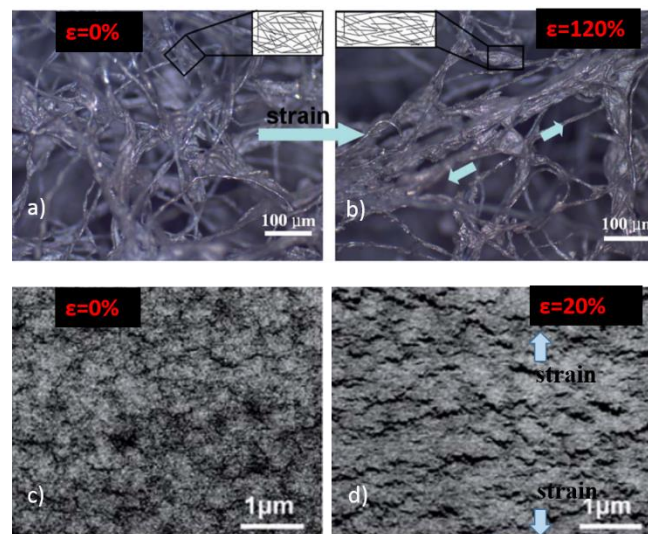


**Figure 2.** (a) and (b) show the effect of elongation on the micro structure of cotton-AgNW network before and under tensile strain [34]. (c) and (d) show the micro-cracks on the Ag NP thin film before and under strain [36].

### 3. CATEGORIZING FACIAL EXPRESSION FEATURES

There are six basic human emotions as defined by Ekman and Friesen in 1978 which comprise of happiness, anger, sadness, surprise, fear and disgust [18]. In vision sensors, the facial expression can be categorized using the Facial Action Coding System (FACS) technique. FACS is a system that was developed based on facial muscle changes where it can characterize facial actions to express a person emotions. In FACS, the movements of specific facial muscles called action units (AUs) as shown in Figure 3(a) that reflect distinctive temporary changes in facial appearance are encoded to assist the human expression recognition [16]. The facial emotions recognition is accomplished by detecting individual AU and the system will eventually classify facial group according to the combinations of the AUs.

For EMG sensors, knowing the muscles responsible for facial expression in details is important to help with the electrode's placement. They must be placed in the most effective area on the face. This is due to the fact that the closer electrodes to the muscles fibre, the higher the voltage amplitude produced by those muscles. The EMG sensors then measure the electrical activity of the motor unit in the striated muscle of the face during facial expression. Figure 3(b) shows the emotional muscles involved in facial gestures which are Frontalis, Pars Medialis (Inner Brow Raiser), Frontalis, Pars lateralis (Outer Brow Raiser), Corrugator supercillii, Depressor supercillii (Brow Lower), Lavator labii superioris (Upper Lip Raiser), Zygomaticus minor (Nasolabial Deepener) and Zygomaticus major (Lip Corner Puller) [24]. For the six universal emotional expressions, facial muscles involved in each of them can be inferred from corresponding action units from FACS shown in Table 1 [27].

On the other hand, the strain sensor categorizes the facial expression based on the changes in the strain on the skin. Across the face, there are several parts that will experience stress and strain due to facial expression. In most of the reported works, the strain sensors were attached to the forehead, near the mouth, under the eye and on the neck to sense skin strains induced by muscle movement during expression as shown in Figure 3(c) [40]. In [40], Roh reported that happiness and sadness can be differentiated by the  $\Delta R/R_0$  response of the sensor that is attached on the forehead and near the mouth skin [29].

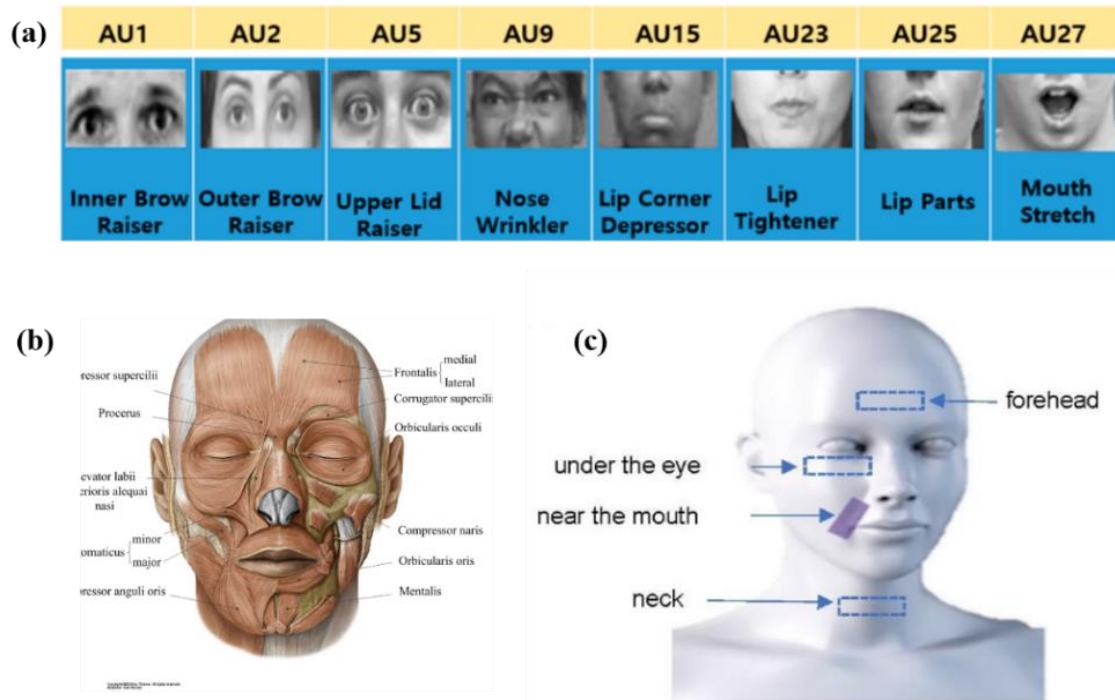


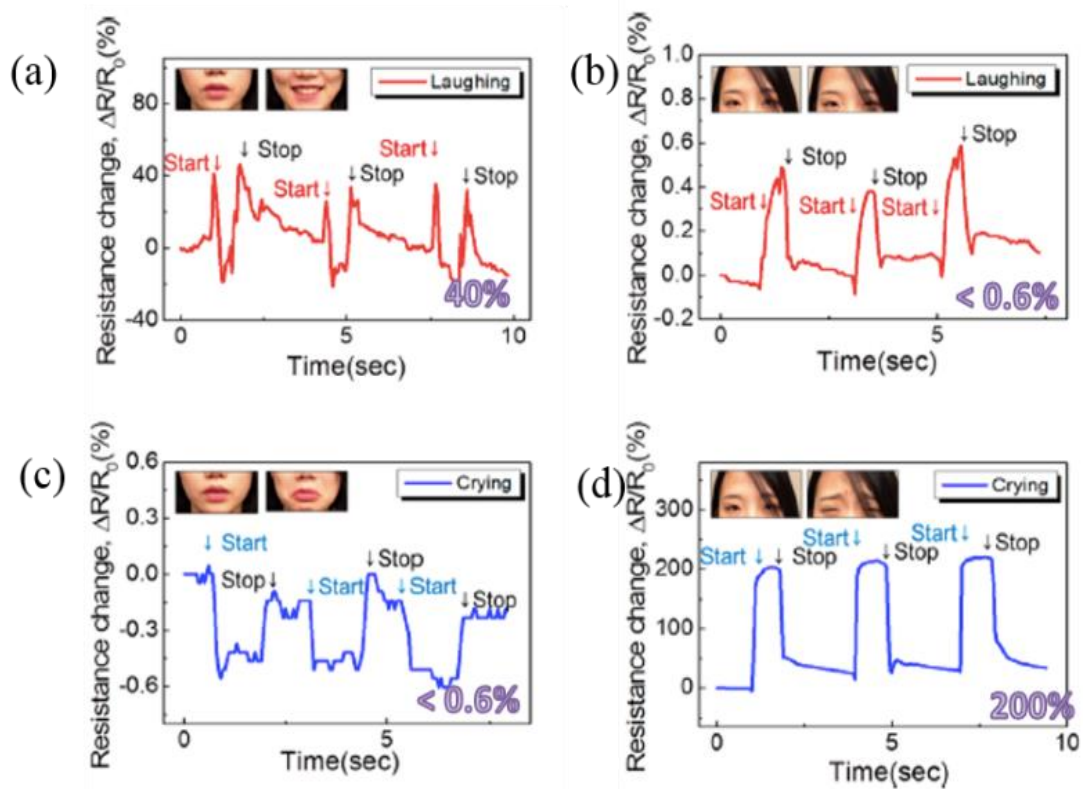
**Figure 3.** Facial expression features. (a) Some of the actions units (AUs) for upper and lower face [17]. (b) Facial muscles [24] and (c) schematic illustration of stretchable transparent ultrasensitive strain sensors attached to the forehead, near the mouth, under the eye, and on the neck to sense skin strains induced by muscle movements during expression of emotions and daily activities [40].

**Table 1** Universal Emotional Expression [24][27]

Expression	Action Units	Action	Facial muscles
Anger	4, 5 or 7, 22, 23, 24	Eyes wide Nostrils lifted compressed mouth Furrowed brow	Corrugator supercilii, Depressor supercilii, Levator palperbrae superioris, Orbicularis oculi, Orbicularis oris
Disgust	7,9,19,25,26	Upper lip raised Lower lip downwards Mouth Open	Levator labii superioris, Levatorlabii superioris alaeque nasi
Fear	1, 2, 4, 5, 7,20,25	Eyes wide Mouth open Eyebrows closed Retracted lips	Frontalis, Depressor supercilii, Levator palperbrae superioris, Risorius
Happiness	6, 12,25,26	Lifted mouth corners Wrinkled under-eye skin Raised cheekbones	Orbicularis oculi, Zygomaticus major
Sadness	1, 4,6,15,17	Slumped mouth corners Drooped eyelids	Frontalis, Depressor anguli oris
Surprise	1, 2, 5, 25 or 26	Eyebrows raised Wrinkled forehead Eyes wide Mouth open	Frontalis, Levator palperbrae superioris Depressor labii, Orbicularis oris

Figure 4 shows that when a person is laughing or smiling, the muscles around the mouth and cheekbone make larger movement than in other facial areas. The resistance change responses  $\Delta R/R_0$  in that area is around 40% compared to the muscle around the forehead which is moved only slightly, 0.6%. In contrast to the sad expression, the muscle on the forehead will experience larger movement which causes the change in resistance to increase up to 200% while the resistance change for the muscle near the mouth is less than 0.6%. On the other hand, Yin et al [41] prefers to place the sensors on the forehead and philtrum of a person. The insight behind this is when the subject cried, the frown on the forehead and the wrinkle of the philtrum caused shrinkage which leads to the decrease of resistance which is around 30%. Meanwhile, when a person laughed, muscle around the forehead and philtrum stretched and caused the increase of the resistance change which are 80% and 10% respectively. Although the change of resistance of the sensor on the forehead is less compared to [15], the placement of the sensor on philtrum gave a better sensitivity than placing around the corner of the mouth. It is anticipated that by putting more sensors around the face such under the chin and nose may increase the accuracy of the facial recognition systems.

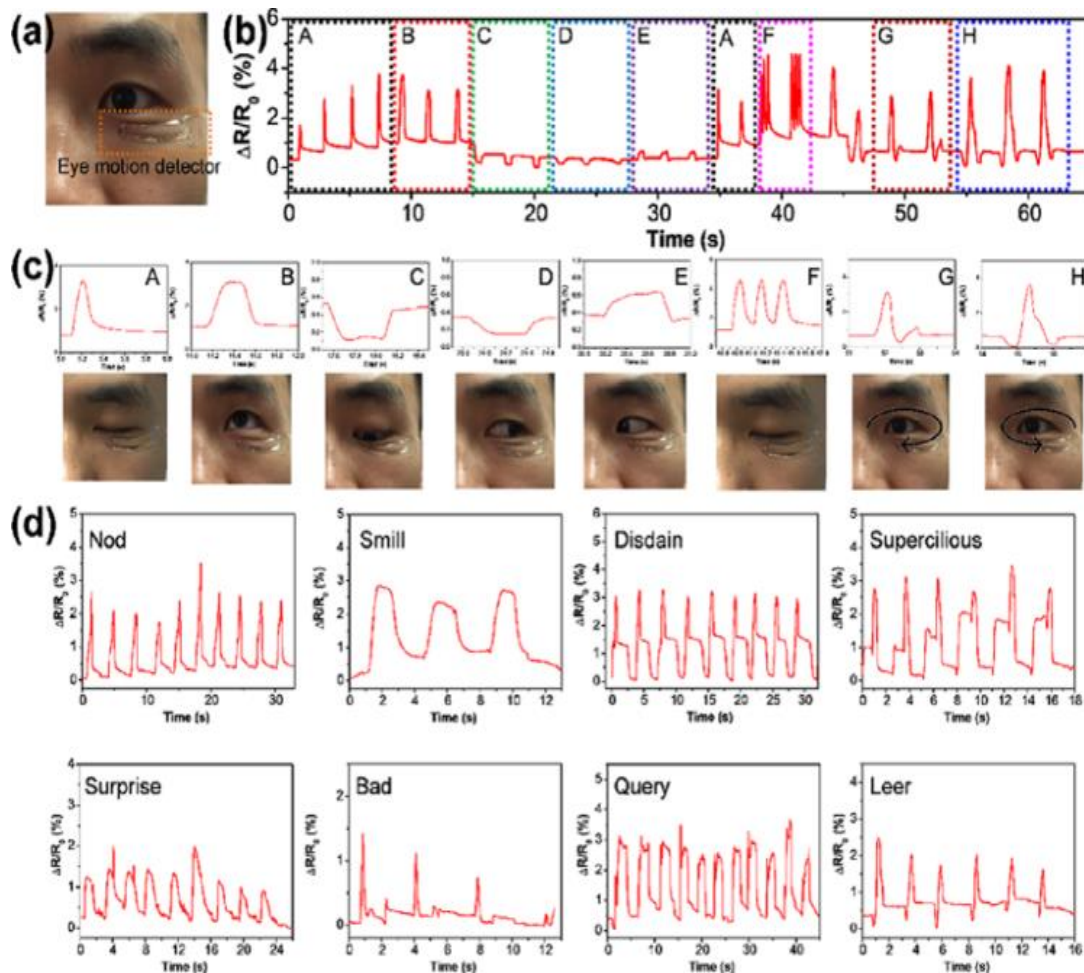
The detection of facial expression can even be more accurate if eyes movement is monitored during the detection process. Highly sensitive strain sensors have the capability to detect the eyes movement such as vibrating, blinking and eye-rolling which is difficult to detect using other sensors such as camera due to minuteness of movement. This eyes movement which produces very small strain can be measured by placing a stretchable and ultrasensitive strain sensor under the eye. Although, the expected change in resistance is small, by monitoring and analysing the signal patterns over a short period of time can help identify the facial expression accurately.



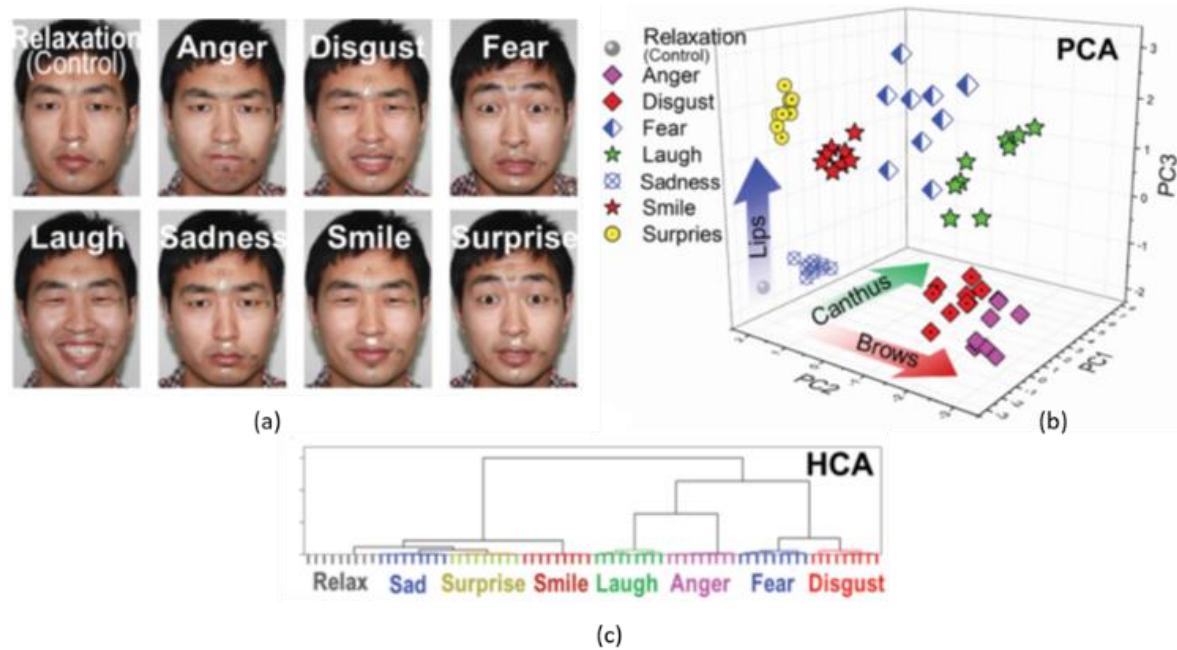
**Figure 4.** Time-dependent  $\Delta R/R_0$  responses of the sensor attached to the (a) skin near the mouth and (b) forehead when the subject was laughing and of the sensor attached on the (c) skin near the mouth and (d) forehead when the subject was crying [41].

Figure 5 shows a strain sensor that is attached to the lower eyelid permitting the detection of the biaxial compression and stretching due to the movements of the eyeball during facial expression. The results show that the resistance signal changes due to the response of the series basic eye movements such as blinking, moving up, down, left and right, and cyclotorsion movement clockwise and anticlockwise. The movement of eyes captured using the sensor can be utilized to predict the emotional expression of a person. Figure 5(d) shows the output signals due to several emotional expressions [42].

Su *et al.* [43] has demonstrated a nanoparticle-based curve array sensor for facial expression recognition which is directly mounted to a human face. The proposed sensors were attached to several locations on the face namely forehead, canthus, philtrum, angulus oris and chin because these regions provide significant muscle movements during facial expression as shown in Figure 6. After obtaining the signals related to the muscle strains, the expression of eight basic emotions which are anger, disgust, fear, laughter, sadness, smiling, surprise and relaxation can be classified using principal component analysis (PCA) and hierarchical cluster analysis (HCA).



**Figure 5.** Application of the strain sensor for emotional expression recognition systems. (a) Photograph of the strain sensor on the lower eyelid. (b) The recorded change in resistance over time for the sensor due to several eye movements shown in (c). (c) Picture of several eye movements and the corresponding close-up views of (b). (d) Signal characteristic of the several facial expression [42].



**Figure 6.** (a) The strain sensors were conformably attached at six different positions on the face to determine several facial expressions. (b) PCA result illustrates a clear grouping of the eight different facial expressions called analytes. (c) HCA shows the similarity clustering of the analytes based on the variation trend of the muscle movement [43].

#### 4. SENSOR DESIGN AND FABRICATION

There are many challenges to be addressed in designing and developing efficient and accurate strain sensor for facial expression. In general, the human face has complex muscle groups and produces low deformation of various expression in addition to having low modulus (140 to 600 kPa). There are several requirements that have to be considered in realizing stretchable sensors. One of the requirements is that sensors must be highly sensitive and stretchable to detect small muscle strain induced during facial expression and movement. Moreover, the proposed sensors must be conformal to the skin, able to be very responsive, able to be easily reproduced on an elastic substrate, self-adhesive, transparent and biocompatible. There are several notable approaches to improve stretchability and sensitivity of the sensing circuits which are; 1) by exploiting novel conductor designs, 2) by choosing suitable materials for the conductor and 3) by fabricating ultra-thin sensor. This section explains in detail the existing designs of strain-based FER sensors in the literature, the materials used and their fabrication methods.

##### 4.1 Design of Strain-based FER Sensors

Several conductor designs have been proposed in the previous works for facial expression strain sensor. In summary, the reported designs are straight line [44][45][36], serpentine [43], U-shaped [42] and crisscross link [46][41]. The straight line conductor is the simplest design which makes it easy to develop and fabricate as shown in Figure 7(a). Moreover, a unidirectional strain can be easily measured and interpreted using the straight-line design compared to other complicated geometry since the direction of the applied strain corresponds to the length of the sensor.

However, if the strain to be measured is very large, the use of straight-line design may not be the best choice due to anticipated breakage. Therefore, to accommodate large strain, conductor patterns such as serpentine shape have been implemented in the strain sensor to increase its

stretchability. This technique was proposed in [43] where nanoparticle (NP) based curve array or serpentine shape was used instead of typical straight configuration for face recognition. The serpentine shape was designed with various ratios of the amplitude (terms as R) to the period length to investigate the change in resistance responses and to improve the flexibility of the devices as shown in Figure 7(b). The nanoparticle-based curves arrays were printed on a PDMS substrate by pillar-patterned template induced printing method with silver nanoparticle ink. These curved arrays were then integrated with various interdigitated golden electrodes. Experiments were conducted to verify the reliability of the sensor where promising results were obtained. The proposed strain sensors were still electrically and mechanically stable even after 1000 cycles of continuous strains with a mere permanent deformation of 5%.

In order to improve the sensing capability of a strain sensor, [42] has proposed a novel arcuate U-shaped strain sensor design as shown in Figure 7(c). The new pattern was suggested to ensure conformal fit of the sensor around the eyelid. The structure of the strain sensor consists of an Au conductive layer, a polyacrylic acid (PAA) adhesive layer and a polyurethane (PU) stretchable layer. The proposed design incorporates breathable feature by utilizing biocompatible medical tape for its stretchable substrate. The main justification of employing skin mountable strain sensors is that it can lead to better adhesion between sensors and human skin hence more accurate signal acquisition can be obtained. Due to its novel design, a high sensitivity sensor with a gauge factor from 7.2 to 474.8 with high stretchability up to 140% was realized in this work. The sensor was attached on the lower eyelid permitting the detection of the biaxial compression and stretching due to the movements of the eyeball during facial expression.

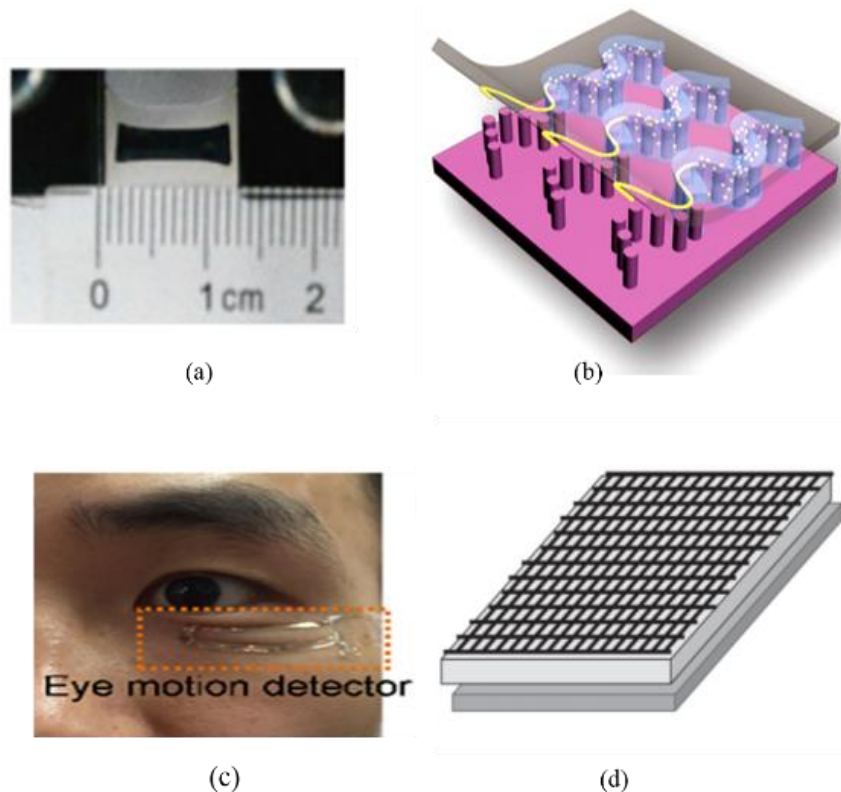


**Figure 7.** Several designs that have been proposed for facial expression strain sensors. (a) Typical straight line. (b) The schematic illustration of the NP curve array (serpentine) were printed on PDMS substrate [43]. (c) U-shape strain sensor. (d) The schematic illustration of crisscross based on GWF strain sensors [46].

Another design that has been proposed to increase the sensitivity of the sensor is crisscross link design [41][46]. Wang *et al.* [46] has demonstrated a crisscross link based on graphene woven

fabrics (GWF) to obtain a high sensitivity face recognition sensor. Figure 7(d) shows the crisscross or tentacle-like pathway configuration based on GWF strain sensor that exhibits a high gauge factor owing to the high-density cracks generated in the network when stress is applied. This can be explained by looking at the effect of stretching on the sensors which cause opening and enlargement of microcrack in thin-film thus limiting the electrical conduction through the thin film which leads to an increase of the electrical resistance. The GF obtained in [46] was 1000 under 2-6% strain, 1000000 under higher strain (>7%) and 35 under small strain 0.2%. As for the sensor developed in [41], the GF are 416 and 3667 within 0%-4% and 48%-57% strain respectively.

Apart from that, a stretchable and patchable strain sensor made of a sandwich-like stacked piezo resistive nanohybrid film of single-wall carbon nanotubes (SWCNTs) and a conductive elastomeric composite of polyurethane (PU)-poly (3,4-ethylenedioxythiophene) polystyrenesulfonate (PEDOT:PSS) on PDMS substrate was reported in [40]. The SWCNTs inserted in the middle of the device act as a bridge to connect the conductive PEDOT to the PEDOT phase. Insertion of SWCNTs layer between PEDOT to PEDOT layers makes the electrical transport becomes more effective and thus improving the sensor's sensitivity. This structure provides a high sensitivity of 62 and high stretchability of up to 100% which can be used to detect small strains induced by emotional expressions such as laughing, crying as well as eye movement.

## 4.2 Sensor Materials

Besides manipulating the conductor design, the choice of substrate materials also a crucial factor in realizing stretchable and wearable strain sensors. Flexible thermoplastic polymers such as polyethylene terephthalate (PET), polycarbonate (PC), polyurethane (PU), Polyethylene naphthalate (PEN), Polyimide (PI) have been widely used for the fabrication of flexible material due to the outstanding optical transparency and high deformability. However, these materials cannot be stretched due to their relatively high Young's modulus. With the recent development in polymers, organic and soft elastomeric substrates such as polydimethylsiloxane (PDMS) and Ecoflex Dragon Skin have been widely adopted to form stretchable and transparent electronics for various purposes including facial expression strain sensors [44][46][47]. PDMS has intrinsic stretchability (up to 1000%), non-toxic, no flammability, hydrophobicity and good processability. Meanwhile, Ecoflex which is also a skin-safe silicone has better stretchability (up to 900%) [48] and lower Young's modulus. These stretchable substrates are able to withstand high mechanical strain while still maintaining their elastic properties [49]. Besides that, textile and fibre are also highly desirable for stretchable substrates due to their similar characteristics to PDMS and Ecoflex. By transforming the textile into conductive material, highly sensitive stretchable devices can be obtained. For example, a highly conductive carbonized pristine plain cotton (CPCF) has been realized by using annealing method at 900°C under an inert atmosphere. Pristine plain weave cotton that consists of dozens of cellulose fibres release small molecules such as H<sub>2</sub>O, CO<sub>2</sub> and CO after being subjected to high-temperature treatment. This process causes the cotton to turn into carbon with distorted graphite structure. After the carbonization process, the textile became thinner and smaller where its size and weight reduced by 49.2% and 84.7% respectively [50].

The performance of the strain sensor in terms of its sensitivity and stretchability can also be improved by engineering a new composite or material for the conductor. Therefore, a lot of studies have focused on the use of nanomaterials to improve strain sensors performance, including Carbon Nanotube (CNTs) [51], silver nanowire (AgNWS) [52], Copper nanowire (CuNW) [53], gold nanowire (AuNW)[54], graphene nanosheets, graphene foam [55], carbon black particles, silver nanoparticles (AgNP). Table 2 and 3 show the summary of typical materials used as substrates and conductors in stretchable devices [56].

To enhance the performance of the conducting materials, the combination of the structures and materials such as carbon nanotubes and silver nanoparticles (CNTs/AgNP)[47], carbon nanotubes with poly(3,4-ethylenedioxythiophene):polystyrene sulfonate and polyurethane (CNTs/PEDOT:PSS/PU) [40], polyacrylic acid and polyurethane (PAA/PU) [42], (PU/CPC) [57] have been proposed. This method provides high stretchability for conformal integration with the curvilinear surface of a human body, hence enhancing mechanical and electrical properties of the sensors [40], [42], [57].

A hybrid conductor design was developed in [58] by mixing two different materials with the aim to better enhance the stretchability of the conductors. The combination of soft and hard networks such as gold nanowire (AuNW) and silver nanowire (AgNW) produces high conductivity, transparency, and stretchability which are difficult to achieve if only using a single type of nanowire. The highly stretchable hybrid conductor was integrated on PDMS where the sensitivity of the PDMS/AgNW/(AuNW) sensor based on GF is 236.6 at low strain ( $\leq 5.0\%$ ) with the maximum stretchability of up to 70% strain. Moreover, the sensing performance of the sensor could be further improved by using thinner substrates to obtain better conformal contact with the skin.

A low modulus and high stretchability strain sensor were demonstrated in [45] using polyvinyl alcohol PVA/polydopamine PDA hydrogel. PVA/PDA hydrogel was obtained by blending certain quantities of aqueous solution of PVA, PDA and sodium tetraborate. PDA was introduced in the composite to enhance skin adhesive and to make it more conformal to the skin. Afterwards, a piece of PVA/PDA hydrogel was encapsulated between two acrylic tapes. The hydrogel can adapt well to the topology of human skin which has an irregular surface to accommodate the movements of limbs and deformation of human skin. This sensor not only has high stretchability up to 75% which is needed to detect large motion but it also can distinguished microstrain (0.1%-0.5) for pulse beating detection. In the face recognition test, it was able to differentiate between a big smile and a shallow smile where the relative change of resistance are 1.3 and less than 1.05, respectively. Moreover, it has a self-healing mechanism which can be explained by the reversible boron ester bond formed between hydroxyl of PVA and borax of sodium tetraborate.

**Table 2** Substrates Used in Stretchable Devices [56]

Materials	Young Modulus (MPa)	Tensile strain	Poisson's ratio
Polyethylene terephthalate (PET)	2,000–4,100	<5	0.3–0.45
Polycarbonate (PC)	2,600–3,000	<1	0.37
Polyurethane (PU)	10–50	>100	0.48–0.49999
Polyethylene naphthalate (PEN)	5,000–5,500	<3	0.3–0.37
Polyimide (PI)	2,500–10,000	<5	0.34–0.48
Polydimethylsiloxane (PDMS)	~ 0.36–0.87	>200	0.49999
EcoFlex	~ 0.02–0.25	>300	0.49999
DragonSkin	1.11	>300	0.49999

A highly stretchable ( $\epsilon=400\%$ ) and highly sensitive resistive type strain sensors with GF of 1678 for facial expression recognition systems were presented in [44]. In order to increase the sensitivity of the sensors, the conductor was synthesized by mixing several brittle metal nanowires (AgNWs, CuNWs, or CNTs) and a conductive organic solution, poly (3,4-ethylenedioxythiophene):polystyrene sulfonate (PEDOT:PSS). Due to the brittleness of the nanowires, it provides an outstanding sensitivity under a small stretchable load. In addition, the use of conductive organic solution significantly enhances the deformation endurance of the device.

**Table 3** Conductive materials for stretchable sensing devices [56]

Conductive Materials	Structure/form	Size	Sheet Resistance
Metallic nanomaterials (Ag, Au, Cu, Al, Mn, Zn)	Nanoparticles, nanowire, nanorods	2–400 nm (in diameter) and 200–1000 nm (in length)	0.015–20 $\Omega$ sq <sup>-1</sup>
Carbon-based nanomaterials (e.g., CNTs, graphene)	Nanoparticles, nanowires, nanotubes, nanofibers	10–2000 nm (in diameter) and 500–5000 nm (in length)	30–5×10 <sup>6</sup> $\Omega$ sq <sup>-1</sup>

### 4.3 Fabrication Methods

The fabrication procedure of flexible or stretchable sensors need to be low-cost and scalable if the technology is to be envisioned for wide implementation of facial expression recognition systems in the future. Various fabrication techniques have been developed and proposed over the years to fabricate a number of facial expression recognition strain sensors. Based on the literature, there are several widely used fabrication techniques for fabricating strain-based FER sensors which are solution-phase [45][44][59], dip coating techniques [32][57], drop-casting [43][58][60], spray coating [61], and screen printing [35]. In general, these techniques are mainly used since they can accommodate low melting point and high hydrophobicity of soft elastomeric substrate for FER strain sensors. Moreover, the deposition process using microfabrication technology was also implemented for developing FER strain sensors such as e-beam evaporation [42] and chemical vapour deposition (CVD) [46]. It has also been reported that carbonization method was used to realize conductive textile strain sensors by exposing materials such as cotton, silks, wools and sponge to high-temperature treatment [62][63][50].

#### 4.3.1 Solution Phase Method

Solution phase technique is the most common method used to fabricate stretchable facial expression strain sensors as reported in the literature mainly due to its simple fabrication process [45]. Solution phase method or liquid phase mixing is a process where different materials are mixed to produce composite stretchable and conductive materials. Liu *et al.* [45] prepared (PVA/PDA) hydrogel by mixing PVA, PDA and sodium tetraborate. The homogenous hydrogel was formed by adding a PDA solution to 10wt% PVA aqueous solution with stirring, where it was then immediately added with sodium tetraborate under intense agitation (300rpm). The mixture was then stirred continuously for 5 minutes.

Han *et al.* [44] have produced a nanowire–microfluidic hybrid (NMH) strain sensor by utilizing different nanowires microchannel structure. Firstly, a microchannel is crated and coated with nanowire (AgNWs, CuNWs, or CNTs) before injecting a conductive organic solution poly(3,4-ethylenedioxy-thiophene):polystyrene sulfonate (PEDOT:PSS) into the channel. The combination of the two materials produced a sensor with outstanding sensitivity under small stretchable load due to the brittleness of the nanowires while the use of conductive organic solution helps to sustain the deformation of the device under strain.

#### 4.3.2 Dip Coating Techniques

One of the methods to synthesize ultra-thin films is by implementing dip coating techniques. This technique is based on dipping a substrate into a solution at a controlled rate. The advantage of the dip-coating technique is that it can produce a very thin layer with good uniformity. However, the coating will be deposited on both sides of the substrate due to being immersed in the solution.

Wu has successfully demonstrated in [57], a highly sensitive strain sensor based on ultrathin conductive polymer composites (CPC) layer-decorated polyurethane (PU) yarn using dip coating techniques. The PU yarn was coated with negatively charged carbon black (CB)@cellulose nanocrystals (CNC)/natural rubber (NR) nanohybrid to form an ultrathin conductive CPC layer via layer-by-layer (LBL) assembly process using positively charged chitosan (CS) as a mediator. Figure 8 shows the schematic diagram of the CPC@PU yarn strain sensor. The conductivity of the sensors was improved using two different methods which are by increasing the content of conductive filler in the CPC layer and the LBL numbers of CPC layer. Afterwards, the CPC@PU yarn segment was bonded on a PDMS layer. This sensor has shown high sensitivity with a gauge factor (GF) of 39 and a detection limit of 0.1% strain with good reproducibility of over 10000 cycles.

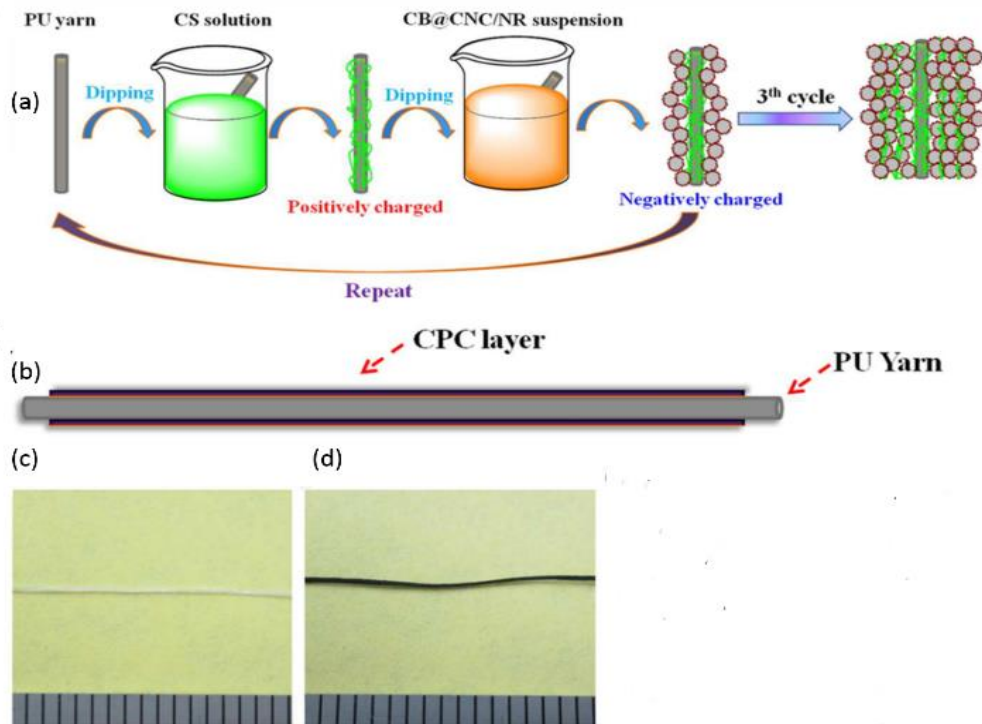


**Figure 8.** (a) Schematic illustrations for preparation of the CPC@PU yarn using LBL assembly technique. (b) Structural schematic diagram of the CPC@PU yarn strain sensor. (c) Photographs of neat PU yarn (d) and CPC@PU yarn [57].

### 4.3.3 Drop-Casting Method

Drop-casting process is carried out by dropping off a solution onto the substrate and waiting for the solvent to evaporate. The film thickness obtained depends on the concentration of the solution. The main advantage of this method is the ease of fabrication while the main drawbacks are difficulty in controlling the thickness of the layer and poor uniformity, especially for a large fabrication area.

Ho *et al.* [58] demonstrated that the combination of a rigid and soft network such as AgNWs and AuNWs can be fabricated using the inexpensive drop-casting method. The process starts with AgNWs being dropcast onto PDMS substrate and subsequently followed by the deposition of AuNWs on top of the AgNWs layer. To ensure uniform deposition of hydrophobic AuNWs on the top of AgNW is achieved, Langmuir transfer is adopted.

Besides that, Su *et al.* realized FER system using the same method by drop casting AgNP on a pillar-patterned template as developed in [43]. The process starts with the development of a pillar-patterned silicon template with a radius of 5  $\mu\text{m}$  and a height of 20  $\mu\text{m}$ . Afterwards, 10  $\mu\text{L}$

droplet of AgNP/sodium dodecyl sulfate (SDS) hybrid suspension was dropped onto the template and subsequently covered by a PDMS film where AgNP curves will be eventually printed on the film. To complete the fabrication process of the AgNP curve arrays, the film is sintered at 200°C for 2 hours. In the final stage of the process, Cr/Au interdigitated electrodes are integrated onto the film to produce a highly sensitive and full integrated strain sensor. Figure 9 shows the schematic illustration of the nanoparticle self-assembly process induced by a pillar pattern template.

#### 4.3.4 Spray coating

Another type of deposition method that has been used for FER strain sensor is a spray coating technique. Generally, the spray coating technique is a transformation of a liquid precursor solution into a fine aerosol by atomizer or nebulizer. The spraying solution is deposited on a substrate surface either through with carrier gas or with electrostatic field or by gravity. Generally, spray coating techniques can be categorized into three; electrostatic spray deposition (ESD), pressurized spray deposition (PSD) and spray pyrolysis technique [64]. The morphology of the films produced is different based on the spray technique used. Besides that, parameters such as flow rate, substrate temperature and deposition time will affect the morphology of thin films. Cracks may form if the flow rate exceeds a certain value for a particular composition of the solution and associated parameters. Lei Zhang *et al* have realized FER sensor that comprises of silver nanoparticle and reduced graphene oxide (Ag rGO) using spray coating technique [61]. First, AgNWs is spray-coated on the PDMS surface substrate at 75°C as an electrode and followed by deposition of Ag rGO thin film by using the same method. In a nutshell, spray coating is a very simple and cost-effective technique. Large coverage area, adjustable layer thickness, and independent of substrate topology are the advantages of spray coating.

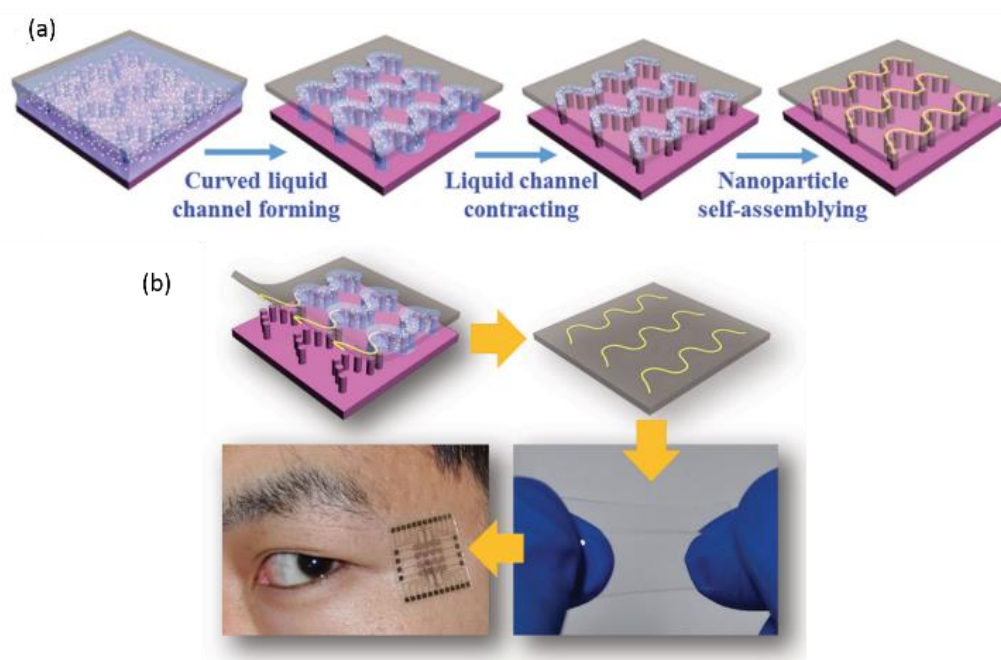


**Figure 9.** (a) The schematic illustration of the nanoparticle self-assembly process induced by pillar-patterned template using drop casting method. (b) The schematic illustration of the NP curve array printed to flexible electronic devices and implemented to multianalysis for skin micro-motion sensing [42].

### 4.3.5 Screen Printing Method

Printing method is a simple and cost-effective approach that can be applied for patterning nanomaterial and other conductive materials for stretchable and flexible electronic devices. Several printable functional materials have been developed and optimized for traditional printing methods such as screen printing [65], inkjet printing [66], [67], and roll-to-roll (R2R) printing to achieve stretchable conductors. Among these printing types, screen printing technique is the simplest way to pattern and deposit various materials on different substrates without sophisticated equipment or clean room. The equipment involves for screen printing is a squeegee or fill blade to force functional ink into the mesh or opening of the screen where the transfer of the desired pattern onto the surface of the chosen substrate takes place. The pore mesh range is between 10-200  $\mu\text{m}$  [68]. Even though screen printing technique has the capability to print single or stacked layers on to variety of soft material such as textile and plastic films, limited selection of ink materials and low printing resolution ( $>10 \mu\text{m}$ ) makes it difficult to realize complex geometries.

Tolvenan *et al.* [35] has proposed a screen printing method to develop a novel strain sensor for the purpose of facial expression recognition. The proposed sensor functions by exploiting a cracking structure of silver ink patterned silicone elastomer-silver plated nylon structure (Ag-DS/CF). A conductive fabric (CF) was cut into two T/L shape structures and was secured onto the bottom of a mould using double-side tape. Then, several pieces of Kapton tape (KT) of size 5 mm  $\times$  1 mm  $\times$  0.2 mm were placed between the T/L shaped conductive fabrics to form a cavity as shown in Figure 10. A specific mixture of silicone elastomer (Dragon Skin, DS) was poured into the mould to cover the CF/KT structure and was left to dry at room temperature for 75 minutes. The DS/CF structure was detached from the mould and KT. In order to generate wrinkle Ag pattern, the silver ink was screen printed into the cavity created earlier in pre-stretching condition and baked at 120°C for 10 minutes. Afterwards, the Ag-DS/CF was over-moulded with another layer of DS to cover the cavity and the sample was left to dry for several hours at room temperature. Finally, Skin Tite silicon was put at the backside of the sensor to act as an adhesive layer.

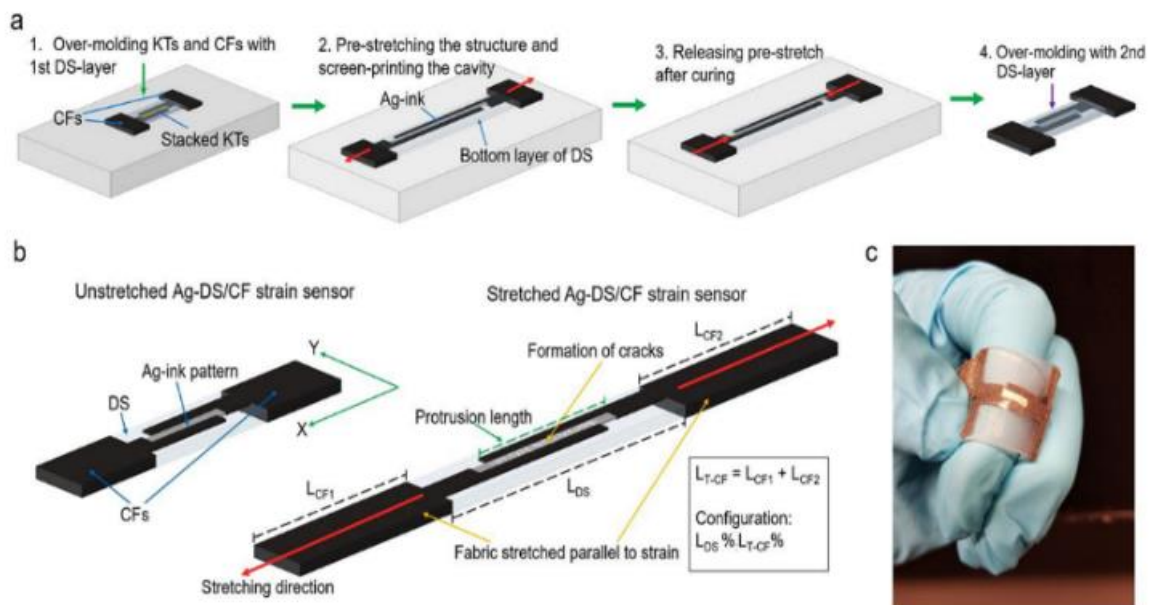


**Figure 10.** (a) Fabrication processes of Ag-DS/CF strain sensors. (b) Unstretched Ag-DS/CF strain sensors. (c) Stretched Ag-DS/CF strain sensors [35].

#### 4.3.6 E-beam Evaporation Method

On the other hand, the deposition method via e-beam evaporation technique from microfabrication process has been used to fabricate the conductor layer of facial expression recognition strain sensor in [42]. E-beam evaporation technique is a physical vapour deposition where the target material that is used as coating layer is bombarded with an electron beam from a charged tungsten filament to evaporate and convert it to gaseous for deposition on the material to be coated [69]. These atoms or molecules in a vapour phase then form a thin film coating on the substrate under a high vacuum chamber. Figure 11(a) shows the fundamental structure of the strain sensor which consists of Au conductive layer, polyacrylic acid (PAA) adhesive layer and polyurethane (PU) film. PAA adhesive layer is used as biocompatible medical tape while the PU film layer is chosen as a stretchable elastomeric substrate. In order to strengthen the binding force between the substrate and the conductor, the PU layer is pre-treated with oxygen plasma. Then, the Au conductive layer is blanket deposited using e-beam onto the PU layer to form a stretchable conductor. The device can then be cut into a desirable shape. Silver paste is coated on the two edges of the conductive layer to provide electrical connection for measurement purposes. Figure 11(b) shows the cross-sectional of scanning electron microscopy (SEM) image of the strain sensor attached on medical tape which indicates that the whole thickness of the strain sensor is 48  $\mu\text{m}$ . The fabricated strain sensor is conformably attached to the lower eyelid shown in Figure 7(c). The main advantage of e-beam evaporation technique is it allows high deposition rate and evaporation of high-temperature materials and refractory metals such as tungsten, tantalum, or graphite [69]. However, e-beam evaporation method requires the use of a clean room which is not widely accessible.

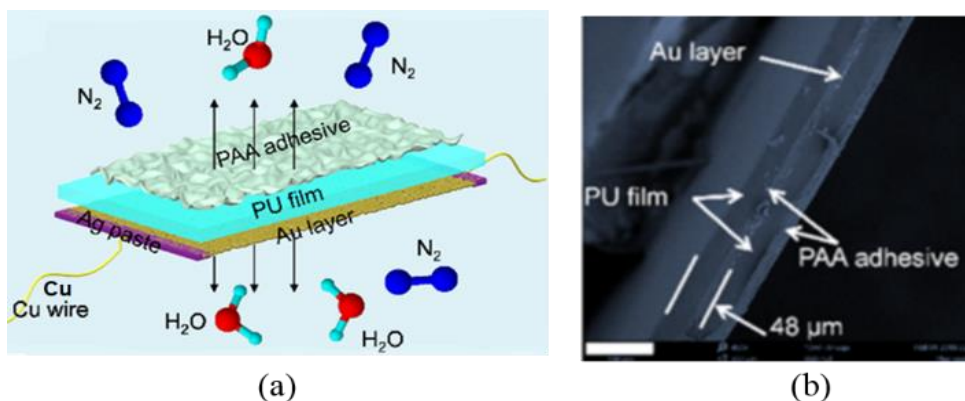


**Figure 11.** (a) Cross-sectional SEM image of the strain sensor attached on medical tape. (b) Cross-sectional SEM image of the strain sensor attached on medical tape [42].

#### 4.3.7 Chemical Vapor Deposition (CVD)

FER strain sensor has been realized using chemical vapour deposition CVD method in [46]. Chemical vapour deposition is a process which materials are deposited or grown from the vapour phase by the decomposition of chemicals on the surface of a substrate which is controlled by a chemical reaction. CVD is widely used in microfabrication process to deposit materials including silicon (dioxide, carbide, nitride, oxynitride), filaments, tungsten, titanium nitride, high-k dielectric and carbon (fibre, nanofiber, nanotube, diamond and graphene). This technique can produce uniform thickness and properties with low porosity even on substrates of complicated shape. Moreover, it also has the capability of selective deposition on the substrate pattern. For FER strain sensor, Wang *et al.* [46] has grown graphene around the copper mesh using atmospheric pressure chemical vapour deposition (CVD). The graphene woven fabrics (GWFs) were obtained when copper mesh was etched away when immersed in

FeCl<sub>3</sub>/HCl solution. Then GWFs were transferred to PDMS with medical tape to realize FER strain sensor.

#### 4.3.8 Carbonization Method

FER strain sensors can also be fabricated by mean of carbonizing fabric or raw materials such as silk [63], cotton [50] and sponge [70]. Carbonization process is normally carried out through high-temperature pyrolysis process under an inert atmosphere. This process contributes to low cost and large scale production where the sensors demonstrate high linearity and sensitivity. However, this technique requires high-temperature treatment up to 1000°C in a furnace.

Yu *et al.* [62] reported a stable mechanical strain sensor based on carbonized nanosponge (CNS). Commercially available melamine or nanosponge for cleaning was washed with ethanol and deionized water before being carbonized in a tubular furnace at 1000°C for 2 hours in N<sub>2</sub> atmosphere. Then, CNS was washed with ethanol and deionized water to remove impurities. Owing to the 3D network structure, this strain sensor obtained compressive strain within 0-40% with GF up to 18.4, fast response (100 ms) and high stability (>100).

A highly sensitive strain sensor with GF of 416 within 0%–40% strain was successfully fabricated using similar technique [41]. The GWF was fabricated using a cotton bandage as the template which has a feature of a macro woven-fabric structure. The cotton bandage was firstly dip-coated in Graphene Oxide (GO) solution. Afterwards, the composite is transferred to an ethanol flame and exposed for a few seconds to pyrolyze the cotton template and to reduce the GO structure simultaneously. In the final stage of the process, the GWF is encapsulated with natural rubber latex.

Besides that, Wang *et al.* also have demonstrated ultra-sensitive strain sensor which also can be used for FER based on the carbonized silk georgette (CGS) in [63]. The georgette silk was carbonized in argon and hydrogen using a tube furnace. Compared to other fabric such as plain-weave fabric, georgette silk which composed of highly twisted yarn in warp and weft directions produced higher sensitivity and lower detection limit in sensing performance. This strain sensor can reach up to 100% stretchability, GF of 173 and 29.7 for 60%-100% strain and 40% strain, respectively. In addition, the CGS strain sensor also achieved high durability and stability (10 000 stretching cycles at 100% strain), and fast response (<70 ms).

In summary, Table 4 shows the advantages and disadvantages of each fabrication method discussed while Table 5 shows the comparison of performance results of facial expression strain sensors proposed in the literature.

**Table 4** Advantages and disadvantages of different fabrication techniques

<b>Fabrication techniques</b>	<b>Advantages</b>	<b>Disadvantages</b>
Solution phase	<ul style="list-style-type: none"> <li>▪ Low cost</li> <li>▪ Large quantity</li> </ul>	<ul style="list-style-type: none"> <li>▪ Difficulty to control the thickness</li> </ul>
Drop casting	<ul style="list-style-type: none"> <li>▪ Simple</li> <li>▪ No waste of material</li> </ul>	<ul style="list-style-type: none"> <li>▪ Limitations in large area coverage</li> <li>▪ Difficult to control the thickness</li> </ul>
Dip coating	<ul style="list-style-type: none"> <li>▪ Good uniformity</li> <li>▪ Very thin layers</li> <li>▪ Large area coverage</li> </ul>	<ul style="list-style-type: none"> <li>▪ Waste of material</li> <li>▪ Time-consuming</li> <li>▪ Double side coverage</li> </ul>
Screen printing	<ul style="list-style-type: none"> <li>▪ Simple</li> <li>▪ Low cost</li> </ul>	<ul style="list-style-type: none"> <li>▪ Resolution &gt;10µm</li> <li>▪ Limited ink materials</li> </ul>
Carbonization method	<ul style="list-style-type: none"> <li>▪ Low cost</li> <li>▪ High stability and sensitivity</li> </ul>	<ul style="list-style-type: none"> <li>▪ Require high temperature</li> <li>▪ Not suitable for soft elastomeric</li> </ul>
Spray Coating	<ul style="list-style-type: none"> <li>▪ Large area coverage</li> <li>▪ Adjustable thickness</li> </ul>	<ul style="list-style-type: none"> <li>▪ Homogeneity of the film</li> </ul>

	<ul style="list-style-type: none"> <li>▪ Independent on the substrate</li> </ul>
E-beam	<ul style="list-style-type: none"> <li>▪ High deposition rate</li> <li>▪ Require clean room</li> <li>▪ High cost</li> </ul>
CVD	<ul style="list-style-type: none"> <li>▪ Conformal large-area growth, reproducibly very high levels of purity in the as-grown materials.</li> <li>▪ Require clean room</li> <li>▪ High cost</li> </ul>

**Table 5** Summary of performance results of facial expression strain sensors

Paper	Type of strain sensor	Design/ Structure	Material	Fabrication	Stretchability (% strain)	Sensitivity of Gauge Factor (GF)
[43]	Resistive	Curved array conductor (serpentine)	AgNp -PDMS	Drop casting Pattern: Pillar patterned template	5%	-
[46]	Resistive	Crisscross link	GWF- PDMS, and medical tape.	CVD Pattern: Copper mesh	30%	≈1000 under 2–6% strains, 1000000 under higher strains (>7%), ≈35 under small strain of 0.2%.
[40]	Resistive	Straight line	SWCNTs- PEDOT:PSS/P U- SWCNTs	Solution phase based Pattern: None	100%	62
[41]	Resistive	Crisscross link	GWF	Dip coating /Carbonization Pattern: Cotton bandage template	57%	416 within 0%–40% strain 3667 within 48%–57% strain
[42]	Resistive	U-shape	Au - PAA -PU	E-beam evaporation Pattern : None	140%	7.2 to 474.8
[58]	Resistive	Straight line	PDMS- (AuNW)- (AgNW)- PDMS)	Drop casting Pattern: None	70%	≈236 at low strain (<5%)
[47]	Resistive	Straight line	CNT- AgNP- PDMS	Solution phase Pattern: Trench on PDMS substrate	3.2%	2.5
[57]	Resistive	Straight line (Yarn)	CPC@PU yarn	Dip coating Pattern: Based on yarn structure	0.1%	39
[44]	Resistive	Straight line	AgNWs/CuNWs/ CNTs)- (PEDOT:PSS)	Solution phase (microchannel) Pattern: Polyimide tape	4%-6% 6%-10% to over 10%-16% 400%	8 10, 30 1678
[45]	Resistive	Straight line	PVA/PDA hydrogel	Solution phase	0.1%-75%	-
[71]	Resistive	Straight line	Multiple hydrogen bonding elastomer (MBHE);	Solution phase	0-10%	-

			Carboxyl cellulose nanocrystals(CNC)/chitosan (CT)/decorated epoxy natural rubber (ENR)			
[59]	Resistive	Straight line	Standing enokitake-like gold-nanowire-based films chemically bonded to an elastomer	Solution phase		-
[35]	Resistive	Straight line	Ag-DS/CF	Screen printing Pattern: Kapton tape	7 to 75%	10 <sup>4</sup> -10 <sup>6</sup>
[50]	Resistive	Straight line	Carbonized pristine plain cotton (CPCF)	High temperature treatment (annealing)	0 to 80% 80% to 140%	GF = 25, GF = 64, Can detect as low as 0.02%
[60]	Resistive	Straight line	AuNW-latex	Drop casting	0.01% and 350%,	GF=6.9 to 9.9
[61]	Resistive	-	Ag-rGO (Ag particles - Graphene Oxide), PDMS substrate.	Spray coating	≤ 200% < 0.2%	GF = 429, GF = 7.23,
[62]	Resistive	Straight line	Carbonized nano sponge (CNS)	High temperature treatment (annealing)	0-10% 10%-25% 25-40%	GF=4.3 GF=18.4 GF= 8.4
[63]	Resistive	Straight line	Carbonized Georgette Silk (CNS)	High temperature treatment (annealing)	0-40% 60-100% Can detect as low 0.01%	GF=29.7 GF=173

## 5. POTENTIAL APPLICATIONS

Facial expression recognition technology can be used in a wide range of applications such as in biomedical, gaming, human-machine interaction and security. Depending on the nature of the application, a suitable detection technique can be chosen from a number of methods described in the previous sections. For example, human micro facial expression can be detected by using an EMG based sensor [72][73]. For instance, the ability of the system to accurately detect micro-facial expression is very valuable in the field of psychology and security where a person may attempt to conceal or suppress their true emotion during interrogations.

### 5.1 Biomedical Applications

One of the main areas where facial expression recognition systems could thrive is in the biomedical field. As the world is embracing technology in the healthcare sector, the number of

potential applications in this sector is increasing tremendously. One of the applications is to utilize facial expression recognition as an effective tool in behavioural studies and medical rehabilitation. By monitoring patients' facial expression and muscle fatigue information remotely, a system has been developed to modify their training modes online [74]. For instance, the damping of a treadmill can be adjusted automatically based on the patients' expression and muscle fatigue as shown in Figure 14. In general, a patient with positive expression and without fatigue will see an increase in difficulties of the exercises while a patient that shows negative expression and mild fatigue will have more relaxing exercises. In addition, development of automatic recognition systems for emotional status based on facial expression will vulnerable such as patients who experience mental issues, patient with depression and children with less ability to control themselves such as autism. This will help doctors, caretaker, therapist or family to control, understand and take appropriate actions [72].

## 5.2. Human-Computer Interfaces and Robotics

Facial expression recognition is one of the important fields of study for human-computer interface (HCI). A lot of HCI systems have been developed recently to improve human's life quality especially for people with disability. For example, people who suffer from severe motor and disability experience great difficulty to control electric wheelchairs (EWC) [8][75][76]. To address this issue, [8] has proposed a human-computer interface that is capable to distinguish facial expression which then is utilized to control an EWC. This system permits patients to control their wheelchair without having to use their hand. Nine facial expressions such as open mouth or raised eyebrows have been identified and detected by employing a camera as a sensor. The system tracks the face expression and interprets its respective command. In addition, HCI may also allow the patients to steer the wheelchair by utilizing other kinds of signals such as from EMG and strain sensors.



**Figure 12.** The placement of electrodes on human body [74].

## 5.3 Entertainment Technology

With the advancement in computer games and the ever-increasing popularity of e-sport nowadays, additional features like new input devices have been introduced to complement the traditional controls such as the keyboard, mouse joystick and gamepad. The way of controlling computer games is no longer limited to the hands, but it has been extended to other moving parts of the body such as arms and legs by leveraging motion sensing technologies. Some of the technologies such as Microsoft Kinect2 enables players to control the Xbox 360 using body movements and gestures without touching the control device [77]. Apart from that, facial expression recognition systems can also be used as an input to navigate the keyboard and control the games [2]-[4]. Figure 13 illustrates a head-mounted device (HMD) which has been developed to allow 3D facial performance-driven animation in real-time. This wearable device system applies the combination of strain sensor and RGB-D camera. An ultra-thin flexible strain sensor is used to measure the surface strain signal corresponding to upper face expression

while the camera is used to enhance the tracking in the mouth region and account for inaccurate HMD placement. This device is an ergonomic solution for real-time facial performance sensing.

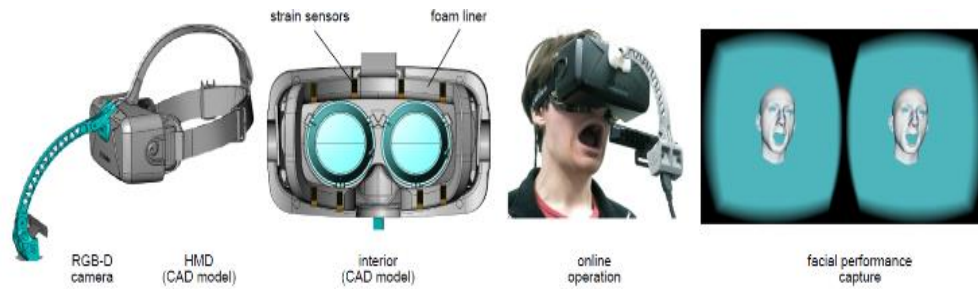


**Figure 13.** Head mounted device for FER [77].

## 6. CHALLENGES AND FUTURE WORK

Based on the review and discussion above, it has been shown that facial expression recognition can play an important role in improving the quality of life in the future. The reported facial expression recognition methods have been applied to various areas ranging from medical applications to gaming. However, there are still a few challenges that need to be addressed. One of the main issues of the facial expression recognition system is the accuracy in detecting the facial expression due to the subtle muscles change which requires highly sensitive and soft sensors. Another major challenge in realizing a complete FER strain sensor systems is in packaging the sensors together with the required power, data acquisition, communication and signal processing. At the moment, most of the reported works employed conventional data acquisition systems via rigid benchtop measuring equipment and wiring.

Therefore, several efforts can be carried out to address these challenges. To improve the sensitivity of the strain sensors, an introduction of intermediate adhesive layers or new designs of sensors that offers similar mechanical properties to that of the human face can be proposed. One of the examples is the use of soft elastomers such as Ecoflex and PVA/PDA hydrogel with Young's modulus of 125 kPa and 46 kPa respectively which are comparable to that of human skin [29]. As for the packaging issue, a fully wearable and standalone facial expression recognition system with an external circuitry required for other functionalities such as power source, signal acquisition, communication and data storage should be made from flexible and stretchable materials as opposed to the conventional rigid structure made from printed circuit boards (PCB). The realization of flexible electronic circuits can pave the way for a fully wearable system. To achieve these goals, further investigations are required to address this limitation.

## 7. CONCLUSIONS

An overview of facial expression detection sensors for a wide number of applications particularly in medical, robotics and entertainment areas is presented. There are two major techniques that are widely used for facial expression recognition which are vision-based sensors and electrical-based sensors. A greater emphasis was given to strain-based sensors where the materials and fabrication methods proposed by several papers in this field were categorized and compared. Performance comparison of reported strain sensors in the literature was carried out based on several criteria mainly sensitivity, stretchability, materials and fabrication methods. It is foreseen that facial expression recognition technology will have a greater role in many applications in the future such as biomedical, robotics, gaming and security. However, some issues such as accuracy, conformability to the skin and complexity of fabrication methods have to be addressed in the future.

## ACKNOWLEDGEMENTS

This work was supported by the Asian Office of Aerospace Research and Development, Tokyo, Japan: SP18-142-0404 and IIUM, RPDF19-004-0014

## REFERENCES

- [1] J. McNulty, "Game-changing skin-like electronics for stroke patients," vol. 18, no. 3, 2018.
- [2] C. Zhan, W. Li, P. Ogunbona, and F. Safaei, "Facial expression recognition for multiplayer online games," *Jt. Int. Conf. CyberGames Interact. Entertain.*, pp. 52–58, 2006.
- [3] M. Nasrul and A. Chowanda, "Navigation Key Using Face Expression in Endless Game," in *3rd International Conference on Computer Science and Computational Intelligence 2018 Navigation*, 2018, vol. 0.
- [4] L. Hao, T. Laura, and O. Kyle, "Facial Performance Sensing Head-Mounted Display," *Am. Surg.*, vol. 20, no. 12, pp. 1281–1290, 2015.
- [5] I. Doroftei, F. Adascalitei, D. Lefeber, B. Vanderborght, and I. A. Doroftei, "Facial expressions recognition with an emotion expressive robotic head," *IOP Conf. Ser. Mater. Sci. Eng.*, vol. 147, no. 1, pp. 0–11, 2016.
- [6] A. R. Naghsh-nilchi and M. Roshanzamir, "An Efficient Algorithm for Motion Detection Based Facial Expression Recognition using Optical Flow," *J. Eng. Appl. Sci.*, vol. 14, no. August, pp. 141–146, 2006.
- [7] C. Darujati and M. Hariadi, "Facial motion capture with 3D active appearance models," *Proc. 2013 3rd Int. Conf. Instrumentation, Commun. Inf. Technol., Biomed. Eng. Sci. Technol. Improv. Heal. Safety, Environ., ICICI-BME 2013*, pp. 59–64, 2013.
- [8] H. da S. Neto and M. R. Fernandes, "Facial Expression Recognition for Human Machine Interface Application," *Int. Work. Assist. Technol.*, no. May, pp. 197–200, 2019.
- [9] Q. X. Nguyen and S. Jo, "Electric wheelchair control using head pose free eye-gaze tracker," *Electron. Lett.*, vol. 48, no. 13, pp. 750–752, 2012.
- [10] A. Ashraf Abbas, O. Sebetela, L. N. Batleng, B. Parhizkar, and A. H. Lashkari, "Facial Expression Recognition Intelligent Security System for Real Time Surveillance," *World Congr. Comput. Sci. Comput. Eng. Appl. Comput.*, pp. 1–8, 2012.
- [11] C. Shan, S. Gong, and P. W. McOwan, "Facial expression recognition based on Local Binary Patterns: A comprehensive study," *Image Vis. Comput.*, vol. 27, no. 6, pp. 803–816, 2009.
- [12] A. Hernandez-Matamoros, A. Bonarini, E. Escamilla-Hernandez, M. Nakano-Miyatake, and H. Perez-Meana, "Facial expression recognition with automatic segmentation of face regions using a fuzzy based classification approach," *Knowledge-Based Syst.*, vol. 110, pp. 1–14, 2016.
- [13] R. Walecki, O. Rudovic, V. Pavlovic, B. Schuller, and M. Pantic, "Deep structured learning for facial action unit intensity estimation," *Proc. - 30th IEEE Conf. Comput. Vis. Pattern Recognition, CVPR 2017*, vol. 2017–Janua, pp. 5709–5718, 2017.
- [14] P. Lucey, J. F. Cohn, T. Kanade, J. Saragih, Z. Ambadar, and I. Matthews, "The extended Cohn-Kanade dataset (CK+): A complete dataset for action unit and emotion-specified expression," *2010 IEEE Comput. Soc. Conf. Comput. Vis. Pattern Recognit. - Work. CVPRW 2010*, no. July, pp. 94–101, 2010.
- [15] Mehdi Ghayoumi, "A Quick Review of Deep Learning in Facial Expression," *J. Commun. Comput.*, vol. 14, no. 1, pp. 34–38, 2017.
- [16] O. Spindler and T. Fadrus, "Grimace project documentation," 2009.
- [17] B. C. Ko, "A brief review of facial emotion recognition based on visual information," *Sensors (Switzerland)*, vol. 18, no. 2, 2018.
- [18] J. Anil and L. P. Suresh, "Literature survey on face and face expression recognition," *Proc. IEEE Int. Conf. Circuit, Power Comput. Technol. ICCPCT 2016*, pp. 1–6, 2016.
- [19] I. M. Revina and W. R. S. Emmanuel, "A Survey on Human Face Expression Recognition Techniques," *J. King Saud Univ. - Comput. Inf. Sci.*, 2018.

- [20] M. Jabon, J. Bailenson, E. Pontikakis, L. Takayama, and C. Nass, "Facial-expression analysis for predicting unsafe driving behavior," *IEEE Pervasive Comput.*, vol. 10, no. 4, pp. 84–95, 2011.
- [21] S. TIVATANSAKUL and M. OHKURA, "Emotion Recognition using ECG Signals with Local Pattern Description Methods," *Int. J. Affect. Eng.*, vol. 15, no. 2, pp. 51–61, 2016.
- [22] R. Munoz *et al.*, "Using Black Hole Algorithm to Improve EEG-Based Emotion Recognition," *Comput. Intell. Neurosci.*, vol. 2018, 2018.
- [23] L. Bareket *et al.*, "Temporary-tattoo for long-term high fidelity biopotential recordings," *Sci. Rep.*, vol. 6, no. April, pp. 1–8, 2016.
- [24] K. Mahyar Hamedi, Sh-Hussain Salleh, Tan Tian Swee, "Surface Electromyography-Based Facial Expression Recognition in Bi-Polar Configuration," *J. Comput. Sci.*, vol. 7, no. 9, pp. 1407–1415, 2011.
- [25] Lou Benedict P. Ang, E. F. Belen, R. A. Bernardo, E. R. Boongaling, G. H. Briones, and J. B. Coronel, "Facial expression recognition through pattern analysis of facial muscle movements utilizing electromyogram sensors," *2004 IEEE Reg. 10 Conf. TENCON 2004.*, vol. C, pp. 600–603, 2005.
- [26] Y. Chen, Z. Yang, and J. Wang, "Eyebrow emotional expression recognition using surface EMG signals," *Neurocomputing*, vol. 168, pp. 871–879, 2015.
- [27] M. Jiang, A. M. Rahmani, T. Westerlund, P. Liljeberg, and H. Tenhunen, "Facial expression recognition with sEMG method," *Proc. - 15th IEEE Int. Conf. Comput. Inf. Technol. CIT 2015, 14th IEEE Int. Conf. Ubiquitous Comput. Commun. IUCC 2015, 13th IEEE Int. Conf. Dependable, Auton. Se.*, pp. 981–988, 2015.
- [28] N. Nazmi, M. A. A. Rahman, S. I. Yamamoto, S. A. Ahmad, H. Zamzuri, and S. A. Mazlan, "A review of classification techniques of EMG signals during isotonic and isometric contractions," *Sensors (Switzerland)*, vol. 16, no. 8, pp. 1–28, 2016.
- [29] M. Amjadi, K. U. Kyung, I. Park, and M. Sitti, "Stretchable, Skin-Mountable, and Wearable Strain Sensors and Their Potential Applications: A Review," *Adv. Funct. Mater.*, vol. 26, no. 11, pp. 1678–1698, 2016.
- [30] J. Chen *et al.*, "Polydimethylsiloxane (PDMS)-based flexible resistive strain sensors for wearable applications," *Appl. Sci.*, vol. 8, no. 3, 2018.
- [31] C. Yan *et al.*, "Highly stretchable piezoresistive graphene-nanocellulose nanopaper for strain sensors," *Adv. Mater.*, vol. 26, no. 13, pp. 2022–2027, 2014.
- [32] J. J. Park, W. J. Hyun, S. C. Mun, Y. T. Park, and O. O. Park, "Highly stretchable and wearable graphene strain sensors with controllable sensitivity for human motion monitoring," *ACS Appl. Mater. Interfaces*, vol. 7, no. 11, pp. 6317–6324, 2015.
- [33] M. Amjadi, A. Pichitpajongkit, S. Lee, S. Ryu, and I. Park, "Highly stretchable and sensitive strain sensor based on silver nanowire-elastomer nanocomposite," *ACS Nano*, vol. 8, no. 5, pp. 5154–5163, 2014.
- [34] C. H. Zhu, L. M. Li, J. H. Wang, Y. P. Wu, and Y. Liu, "Three-dimensional highly conductive silver nanowires sponges based on cotton-templated porous structures for stretchable conductors," *RSC Adv.*, vol. 7, no. 1, pp. 51–57, 2017.
- [35] J. Tolvanen, J. Hannu, and H. Jantunen, "Stretchable and Washable Strain Sensor Based on Cracking Structure for Human Motion Monitoring," *Sci. Rep.*, vol. 8, no. 1, pp. 1–10, 2018.
- [36] J. Lee *et al.*, "A stretchable strain sensor based on a metal nanoparticle thin film for human motion detection," *Nanoscale*, vol. 6, no. 20, pp. 11932–11939, 2014.
- [37] T. Yamada *et al.*, "A stretchable carbon nanotube strain sensor for human-motion detection," *Nat. Nanotechnol.*, vol. 6, no. 5, pp. 296–301, 2011.
- [38] H. Ning, Y. Karube, Z. Masuda, and H. Fukunaga, "Tunneling Effect in a Polymer-Carbon Nanotube Strain Sensor," vol. 24, pp. 388–406, 2009.
- [39] Alamusu, N. Hu, H. Fukunaga, S. Atobe, Y. Liu, and J. Li, "Piezoresistive strain sensors made from carbon nanotubes based polymer nanocomposites," *Sensors*, vol. 11, no. 11, pp. 10691–10723, 2011.

- [40] E. Roh, B. U. Hwang, D. Kim, B. Y. Kim, and N. E. Lee, "Stretchable, Transparent, Ultrasensitive, and Patchable Strain Sensor for Human-Machine Interfaces Comprising a Nanohybrid of Carbon Nanotubes and Conductive Elastomers," *ACS Nano*, vol. 9, no. 6, pp. 6252–6261, 2015.
- [41] B. Yin *et al.*, "Highly Stretchable, Ultrasensitive, and Wearable Strain Sensors Based on Facilely Prepared Reduced Graphene Oxide Woven Fabrics in an Ethanol Flame," *ACS Appl. Mater. Interfaces*, vol. 9, no. 37, pp. 32054–32064, 2017.
- [42] Z. Song *et al.*, "Breathable and Skin-Mountable Strain Sensor with Tunable Stretchability, Sensitivity, and Linearity via Surface Strain Delocalization for Versatile Skin Activities' Recognition," *ACS Appl. Mater. Interfaces*, vol. 10, no. 49, pp. 42826–42836, 2018.
- [43] M. Su *et al.*, "Nanoparticle Based Curve Arrays for Multirecognition Flexible Electronics," *Adv. Mater.*, vol. 28, no. 7, pp. 1369–1374, 2016.
- [44] S. Han *et al.*, "Multiscale nanowire-microfluidic hybrid strain sensors with high sensitivity and stretchability," *npj Flex. Electron.*, vol. 2, no. 1, p. 16, 2018.
- [45] S. Liu *et al.*, "A compliant, self-adhesive and self-healing wearable hydrogel as epidermal strain sensor," *J. Mater. Chem. C*, vol. 6, no. 15, pp. 4183–4190, 2018.
- [46] Y. Wang *et al.*, "Wearable and highly sensitive graphene strain sensors for human motion monitoring," *Adv. Funct. Mater.*, vol. 24, no. 29, pp. 4666–4670, 2014.
- [47] J. Y. Jeon and T. J. Ha, "Waterproof Electronic-Bandage with Tunable Sensitivity for Wearable Strain Sensors," *ACS Appl. Mater. Interfaces*, vol. 8, no. 4, pp. 2866–2871, 2016.
- [48] F. Pineda, F. Bottausci, B. Icard, L. Malaquin, and Y. Fouillet, "Using electrofluidic devices as hyper-elastic strain sensors: Experimental and theoretical analysis," *Microelectron. Eng.*, vol. 144, pp. 27–31, 2015.
- [49] A. N. Nordin and N. Ramli, "Flexible and stretchable circuits for smart wearables," *J. Telecommun. Electron. Comput. Eng.*, vol. 9, no. 3–8, pp. 117–122, 2017.
- [50] M. Zhang, C. Wang, H. Wang, M. Jian, X. Hao, and Y. Zhang, "Carbonized Cotton Fabric for High-Performance Wearable Strain Sensors," *Adv. Funct. Mater.*, vol. 27, no. 2, 2017.
- [51] T. Kim, B. Park, and J. Kim, "Dramatically Enhanced Sensitivity and Signal-to-Noise Ratio in Nanoscale Crack based Mechano-Sensor Inspired by Spider ' s Receptor," no. c, pp. 699–700, 2016.
- [52] S. Yao and Y. Zhu, "Wearable multifunctional sensors using printed stretchable conductors made of silver nanowires," *Nanoscale*, vol. 6, no. 4, pp. 2345–2352, 2014.
- [53] T. Wang, R. Wang, Y. Cheng, and J. Sun, "Quasi in Situ Polymerization to Fabricate Copper Nanowire-Based Stretchable Conductor and Its Applications," *ACS Appl. Mater. Interfaces*, vol. 8, no. 14, pp. 9297–9304, 2016.
- [54] W. Wu, "Stretchable electronics: functional materials , fabrication strategies and applications," *Sci. Technol. Adv. Mater.*, vol. 20, no. 1, pp. 187–224, 2019.
- [55] Y. R. Jeong, H. Park, S. W. Jin, S. Y. Hong, S. S. Lee, and J. S. Ha, "Highly Stretchable and Sensitive Strain Sensors Using Fragmentized Graphene Foam," *Adv. Funct. Mater.*, vol. 25, no. 27, pp. 4228–4236, 2015.
- [56] Kenry, J. C. Yeo, and C. T. Lim, "Emerging flexible and wearable physical sensing platforms for healthcare and biomedical applications," *Microsystems Nanoeng.*, vol. 2, no. April, 2016.
- [57] X. Wu, Y. Han, X. Zhang, and C. Lu, "Highly Sensitive, Stretchable, and Wash-Durable Strain Sensor Based on Ultrathin Conductive Layer@Polyurethane Yarn for Tiny Motion Monitoring," *ACS Appl. Mater. Interfaces*, vol. 8, no. 15, pp. 9936–9945, 2016.
- [58] M. D. Ho *et al.*, "Percolating Network of Ultrathin Gold Nanowires and Silver Nanowires toward 'Invisible' Wearable Sensors for Detecting Emotional Expression and Apexcardiogram," *Adv. Funct. Mater.*, vol. 27, no. 25, pp. 1–9, 2017.
- [59] Y. Wang *et al.*, "Standing Enokitake-like Nanowire Films for Highly Stretchable Electronics," *ACS Nano*, 2018.
- [60] S. Gong *et al.*, "Highly Stretchy Black Gold E-Skin Nanopatches as Highly Sensitive Wearable Biomedical Sensors," *Adv. Electron. Mater.*, vol. 1, no. 4, p. 1400063, 2015.

- [61] W. Z. Lei Zhanga, Hairong Koua, Qiulin Tana, Guanyu Liub, "High-performance strain sensor based on a three-dimensional conductive structure for wearable electronics," *J. Phys. D. Appl. Phys.*, no. December 2016, pp. 0–22, 2019.
- [62] X. G. Yu *et al.*, "A wearable strain sensor based on a carbonized nano-sponge/silicone composite for human motion detection," *Nanoscale*, vol. 9, no. 20, pp. 6680–6685, 2017.
- [63] C. Wang, K. Xia, M. Jian, H. Wang, M. Zhang, and Y. Zhang, "Carbonized silk georgette as an ultrasensitive wearable strain sensor for full-range human activity monitoring," *J. Mater. Chem. C*, vol. 5, no. 30, pp. 7604–7611, 2017.
- [64] M. Torabi *et al.*, "Chemical Solution Deposition Technique of Thi-Fm Ceramic Electrolytes for Solid Oxide Fuel Cells," *Intech*, 2016. [Online]. Available: <https://www.intechopen.com/books/advanced-biometric-technologies/liveness-detection-in-biometrics>.
- [65] X. Liao *et al.*, "Flexible and printable paper-based strain sensors for wearable and large-area green electronics," *Nanoscale*, vol. 8, no. 26, pp. 13025–13032, 2016.
- [66] N. Adly *et al.*, "Flexible Microgap Electrodes by Direct Inkjet Printing for Biosensing Application," *Adv. Biosyst.*, vol. 1, no. 3, p. 1600016, 2017.
- [67] B. Andò, S. Baglio, S. La Malfa, and G. L'Episcopo, "All inkjet printed system for strain measurement," *Proc. IEEE Sensors*, pp. 215–217, 2011.
- [68] Y. Zhao and X. Huang, "Mechanisms and materials of flexible and stretchable skin sensors," *Micromachines*, vol. 8, no. 3, 2017.
- [69] "ELECTRON BEAM EVAPORATION: OVERVIEW." [Online]. Available: <https://angstromengineering.com/tech/electron-beam-evaporation/>.
- [70] T. Yan, Z. Wang, Y. Q. Wang, and Z. J. Pan, "Carbon/graphene composite nanofiber yarns for highly sensitive strain sensors," *Mater. Des.*, vol. 143, no. 2017, pp. 214–223, 2018.
- [71] J. Cao *et al.*, "Multiple Hydrogen Bonding Enables the Self-Healing of Sensors for Human-Machine Interactions," *Angew. Chemie - Int. Ed.*, vol. 56, no. 30, pp. 8795–8800, 2017.
- [72] A. Gruebler and K. Suzuki, "Design of a wearable device for reading positive expressions from facial EMG signals," *IEEE Trans. Affect. Comput.*, vol. 5, no. 3, pp. 227–237, 2014.
- [73] M. Perusquía-Hernández, M. Hirokawa, and K. Suzuki, "Spontaneous and posed smile recognition based on spatial and temporal patterns of facial EMG," *2017 7th Int. Conf. Affect. Comput. Intell. Interact. ACII 2017*, vol. 2018–Janua, pp. 537–541, 2018.
- [74] J. Wang, W. Wang, Z. G. Hou, X. Liang, S. Ren, and L. Peng, "Towards Enhancement of Patients' Engagement: Online Modification of Rehabilitation Training Modes Using Facial Expression and Muscle Fatigue," *Proc. Annu. Int. Conf. IEEE Eng. Med. Biol. Soc. EMBS*, vol. 2018–July, pp. 2304–2307, 2018.
- [75] Y. Rabhi, M. Mrabet, and F. Fnaiech, "A facial expression controlled wheelchair for people with disabilities," *Comput. Methods Programs Biomed.*, vol. 165, pp. 89–105, 2018.
- [76] P. G. Pinheiro, C. G. Pinheiro, and E. Cardozo, "The Wheelie-A facial expression controlled wheelchair using 3D technology," *RO-MAN 2017 - 26th IEEE Int. Symp. Robot Hum. Interact. Commun.*, vol. 2017–Janua, pp. 271–276, 2017.
- [77] M. Ilves, Y. Gizatdinova, V. Surakka, and E. Vankka, "Head movement and facial expressions as game input," *Entertain. Comput.*, vol. 5, no. 3, pp. 147–156, 2014.

